

Charm Photoproduction Results from E691 The Tagged Photon Spectrometer Collaboration*

J. C. Anjos,³ J. A. Appel,⁵ A. Bean,¹ S. B. Bracker,⁸ T. E. Browder,¹
L. M. Cremaldi,⁴ J. R. Elliott,^{4,a} C. O. Escobar,⁷ P. Estabrooks,²
M. C. Gibney,⁴ G. F. Hartner,⁸ P. E. Karchin,⁹ B. R. Kumar,⁸ M. J. Losty,⁶
G. J. Luste,⁸ P. M. Mantsch,⁵ J. F. Martin,⁸ S. McHugh,¹ S. R. Menary,⁸
R. J. Morrison,¹ T. Nash,⁵ P. Ong,⁸ J. Pinfold,² G. Punkar,¹ M. V. Purohit,^{5,b}
J. R. Raab,^{1,c} A. F. S. Santoro,³ J. S. Sidhu,^{2,d} K. Sliwa,⁵ M. D. Sokoloff,^{5,e}
M. H. G. Souza,³ W. J. Spalding,⁵ M. E. Streetman,⁵ A. B. Stundžia,⁸ M. S. Witherell¹

¹ University of California, Santa Barbara, California 93106

² Carleton University, Ottawa, Ontario K1S 5B6, Canada

³ Centro Brasileiro de Pesquisas Físicas, Rio de Janeiro, Brazil

⁴ University of Colorado, Boulder, Colorado 80309

⁵ Fermi National Accelerator Laboratory, Batavia, Illinois 60510

⁶ National Research Council, Ottawa, Ontario K1A 0R6, Canada

⁷ Universidade de São Paulo, São Paulo, Brazil

⁸ University of Toronto, Toronto, Ontario M5S 1A7, Canada

⁹ Yale University, New Haven, Connecticut 06511

September 1988

*Submitted to Phys. Rev. Lett.



Charm Photoproduction Results from E691

The Tagged Photon Spectrometer Collaboration

J. C. Anjos,³ J. A. Appel,⁵ A. Bean,¹ S. B. Bracker,⁸ T. E. Browder,¹ L. M. Cremaldi,⁴ J. R. Elliott,^{4,a}
C. O. Escobar,⁷ P. Estabrooks,² M. C. Gibney,⁴ G. F. Hartner,⁸
P. E. Karchin,⁹ B. R. Kumar,⁸ M. J. Losty,⁶ G. J. Luste,⁸ P. M. Mantsch,⁵
J. F. Martin,⁸ S. McHugh,¹ S. R. Menary,⁸ R. J. Morrison,¹ T. Nash,⁵
P. Ong,⁸ J. Pinfeld,² G. Punkar,¹ M. V. Purohit,^{5,b} J. R. Raab,^{1,c}
A. F. S. Santoro,³ J. S. Sidhu,^{2,d} K. Sliwa,⁵ M. D. Sokoloff,^{5,e} M. H. G. Souza,³
W. J. Spalding,⁵ M. E. Streetman,⁵ A. B. Stundžia,⁸ M. S. Witherell¹

¹University of California, Santa Barbara, CA 93106, USA

²Carleton University, Ottawa, Ontario K1S 5B6, Canada

³Centro Brasileiro de Pesquisas Físicas, Rio de Janeiro, Brazil

⁴University of Colorado, Boulder, CO 80309, USA

⁵Fermi National Accelerator Laboratory, * Batavia, IL 60510, USA

⁶National Research Council, Ottawa, Ontario K1A 0R6, Canada

⁷Universidade de São Paulo, São Paulo, Brazil

⁸University of Toronto, Toronto, Ontario M5S 1A7, Canada

⁹Yale University, New Haven, CT 06511, USA

Abstract

We present results on the photoproduction of 10000 charmed particles from the 10^8 recorded triggers of Fermilab experiment E691. The total cross-section for the photoproduction of D^0 and D^+ particles (and antiparticles) for $x_F > 0.2$ is measured to be $3.88 \pm 0.06 \pm 0.40 \mu\text{b}/\text{Be nucleus}$ at $\langle E_\gamma \rangle = 145 \text{ GeV}$. We have also measured the relative production of different charmed particles, their p_T^2 and x_F distributions and the energy dependence of the total charm cross-section. The mean p_T^2 is $1.16 \pm 0.04 \text{ GeV}^2/c^2$ and the ratio of charm cross-sections at 200 GeV and 100 GeV is 1.96 ± 0.24 . Results of fits to the x_F distribution are also reported.

Pacs numbers: 13.60.Le, 13.60.Rj

The photoproduction of charm is simply described in leading order QCD by the photon-gluon fusion model (PGF)¹. This model has several attractive features. There is only one structure function involved, viz., the gluon structure function which enters to first order as does the QCD coupling constant α_S . In photoproduction there are no leading particle effects as there are no extra quarks within the photon. Finally, the next-to-leading order corrections are expected to be smaller than for hadroproduction. In addition to the simple description afforded by this model, it is also true that at Fermilab energies, photons produce a factor of 5-10 more charm (as a fraction of the hadronic cross-section) than do hadrons. In this paper we present results on the production and fragmentation of charm.

Our charm production experiment, E691, collected data in 1985 using the Tagged Photon Spectrometer at Fermilab. The photons ranged in energy from 80 to 230 GeV ($\langle E_\gamma \rangle = 145$ GeV), and were incident on a beryllium target followed by a high resolution silicon microstrip vertex detector and a spectrometer.² A review of previous fixed-target charm photoproduction experiments can be found in reference 3.

A study of production mechanisms requires measurement of the energy of each photon. Our photon beam was created by the bremsstrahlung of electrons whose energies were measured both before and after radiating, thereby providing a measurement of the energy of the beam photons ($\sigma_E/E \approx 0.08$). The electron tagging failed for approximately 23% of our charm events due to the combined effect of acceptance, counter inefficiencies and the difficulty of reconstructing multiple showers. These events have been entirely removed from those analyses that depend on the energy measurement.

A total of 10^8 triggers were recorded of which 11% required just the presence of hadronic interactions. The remaining 89% were triggers with a high global transverse calorimetric energy, E_T . Using the interaction trigger events we measured the efficiency of the E_T trigger, for both charm as well as non-charm events, to be $(79 \pm 2)\%$ and $(31 \pm 1)\%$, respectively.

In this study, we pay particular attention to the high statistics modes $D^0 \rightarrow K^- \pi^+$, $D^0 \rightarrow K^- \pi^+ \pi^+ \pi^-$ and $D^+ \rightarrow K^- \pi^+ \pi^+$. We also report some results on the modes $D_s^+ \rightarrow \phi \pi^+$, $D_s^+ \rightarrow \bar{K}^{*0} K^+$ and $\Lambda_c^+ \rightarrow p K^- \pi^+$. (Charge conjugate states are included throughout this paper unless otherwise stated).

The number of events in each mode was determined from the mass distribution by a fit to a Gaussian signal shape plus a linear background in the immediate neighbourhood of the mass peak. For the total charm cross-section ($\sigma_{c\bar{c}}$) measurement we used only events with a charm particle above $x_F = 0.2$. A Monte Carlo simulation based on PGF and the Lund model⁴ for hadronization followed by a detailed simulation of the detector was used to correct for the acceptance. We then corrected for the efficiency of the E_T trigger, the fraction of events when the tagging failed and the experimental downtime. The charm cross-sections were obtained by multiplying the ratio of the number of charm events to the number of hadronic events by the total hadronic cross-section^{5,6} of $861 \pm 40 \mu\text{b}$ per Be nucleus.

Systematic errors in the acceptance (obtained from the Monte Carlo) were estimated by varying the cuts used in isolating charm events. Typical cuts were a 5σ minimum on the separation of charm and primary vertices, a minimum joint Čerenkov probability for particle identification of 20% and the requirement that the charmed particle pass within $80 \mu\text{m}$ of the primary vertex. The Monte Carlo simulation of the detector was tuned to both charm and non-charm data. Particular attention was paid to the per plane tracking efficiencies (within 1% of the data), Čerenkov identification and calorimeter simulations which used shower shapes from data. The agreement between the D^{*+} cross-section measured in two different modes (see table 1a) is further evidence that the MC provided a good simulation of the detector.

Cross-sections for producing charmed particles are listed in table 1. The sum of the D^0 , \bar{D}^0 , D^+ and D^- cross-sections in the range $x_F > 0.2$ was measured to be $3.88 \pm 0.06 \pm 0.40 \mu\text{b}$. Our Monte Carlo, which agrees well with the data in the measured x_F region, predicts that 45% of the cross-section lies below $x_F = 0.2$ giving $7.06 \pm 0.11 \pm 0.72 \mu\text{b}$ per Be nucleus for all x_F . After adding the estimated 21% of the cross-section that goes towards producing other charmed particles (according to our Monte Carlo) and then dividing by 2 we determined $\sigma_{c\bar{c}}$, the cross-section for producing a charm event (2 charm particles/event) to be $4.49 \pm 0.07 \pm 0.46 \mu\text{b}$ per Be nucleus. Since the total hadronic cross-section has an A-dependence⁶ of the form A^α where $\alpha = 0.920 \pm 0.002$ and the incoherent cross-section for J/Ψ production has a similar form⁷ with $\alpha = 0.94 \pm 0.02 \pm 0.03$, we assumed that $\alpha = 0.93$ for our case. This leads to a total charm production cross-section per nucleon of $0.58 \pm 0.01 \pm 0.06 \mu\text{b}$ at $E_\gamma = 145 \text{ GeV}$. (If $\alpha = 1$ were chosen instead, $\sigma_{c\bar{c}} = 0.50 \pm 0.01 \pm 0.05$). These numbers are in good agreement with the measurements of the EMC⁸ and BFP experiments⁹ which, when interpolated to our mean energy, yield $\sigma_{c\bar{c}} = 0.59 \pm 0.08 \mu\text{b}$ and $0.67 \pm 0.11 \mu\text{b}$ respectively. It should be noted the latter are muoproduction experiments and the quoted cross-sections involve extrapolation in both Q^2 and A.

Table 1 also lists the ratio of antiparticles to particles, R, in the measured x_F region, $x_F > 0$. This ratio for all D mesons is 1.075 ± 0.021 . This implies that the amount of associated production (i.e., the fraction of \bar{D} s produced in association with Λ_c^+) at our energies is $7.5 \pm 2.1\%$ (i.e., less than 12% at the 95% CL). Further, we found no significant dependence of R on x_F or beam energy.

The fraction of D^0 from D^{*+} is measured to be $0.32 \pm 0.01 \pm 0.03$, in good agreement with a simple model in which D^* and D mesons are produced in proportion to the number of spin states available (3:1) which predicts 0.29 ± 0.02 for the ratio. Averaging $\sigma(D^0)$ from both the observed D^0 decay modes, the ratio $\sigma(D^+)/\sigma(D^0)$ is measured to be $0.53 \pm 0.02 \pm 0.11$, also in agreement with the above model which predicts 0.41 ± 0.03 . For the above calculations we used a world average of the measurements¹⁰ of the branching ratio of the D^{*+} into the D^0 which we computed to be $55.5 \pm 4.5\%$.

The p_T^2 and x_F distributions and the energy dependence of $\sigma_{c\bar{c}}$ for all D mesons combined were corrected for acceptance and Fermi motion effects. The results are shown in figures 1, 2 and 3. The acceptance correction has a slight dependence (approx. 2%) on the parameters of the Lund fragmentation function⁴ which were varied within their known statistical errors and the Fermi motion corrections were small. The effects of changing our most important cuts have also been included as systematic errors. Since the energy dependence of the total cross-section is obtained by comparing charm events with all hadronic events, uncertainties in the energy dependence of the total hadronic cross-section^{5,6} are also included as systematic errors.

The mean values of p_T^2 measured for the copious modes are reported in table 2 and are found to be in good agreement with the average for all D mesons ($1.16 \pm 0.04 \text{ GeV}^2/c^2$). The $\langle p_T^2 \rangle$ for the D_s^+ and the Λ_c^+ were measured to be 1.30 ± 0.26 and $0.86 \pm 0.21 \text{ GeV}^2/c^2$ respectively. The differential cross-section $d\sigma/dp_T^2$ is displayed in figure 1 and is fit well by the form

$$\frac{d\sigma}{dp_T^2} \sim \exp(-bp_T^2 - cp_T^4) \quad (1)$$

with $b = 1.07 \pm 0.05$ and $c = -0.04 \pm 0.01$. The x_F distributions were fit to the form

$$\frac{d\sigma}{dx_F} = A(1 + \alpha x_F)(1 - x_F)^n \quad (2)$$

and are in good agreement with those generated by the Monte Carlo. The fitted values for the parameters α and n are reported in table 2 and the fit for all D mesons is displayed in figure 2. The values of n for the D_s^+ and Λ_c^+ are 3.8 ± 1.2 and 4.1 ± 0.5 respectively.

The rise of the charm cross-section is quantified as the ratio $\sigma(200\text{GeV})/\sigma(100\text{GeV})$ (see table 2) and was fit by a straight line as shown in figure 3. The observed rise $\sigma(200\text{GeV})/\sigma(100\text{GeV}) = 1.96\pm 0.24$ is consistent with the values 1.65 ± 0.50 and 1.44 ± 0.61 measured by the EMC and BFP experiments respectively.^{8,9} The ratio $\sigma(200\text{GeV})/\sigma(100\text{GeV})$ is 1.3 ± 0.9 for the D_s^+ and also 1.3 ± 0.9 for the Λ_c^+ .

In conclusion, we have measured the cross-section for photoproduction of D^0 and D^+ particles (and antiparticles) at $\langle E_\gamma \rangle = 145$ GeV to be $3.88\pm 0.06\pm 0.40$ μb , from which we deduce the per nucleon charm production cross-section to be $0.58\pm 0.01\pm 0.06$ μb . The mean p_T^2 of D mesons is measured to be 1.16 ± 0.04 GeV^2 and the parameter n in the x_F dependence of the cross-section (see expression 2) is measured to be 2.95 ± 0.22 . We have also measured the charm cross-section as a function of E_γ and find a rising dependence quantified as $\sigma(200\text{GeV})/\sigma(100\text{GeV}) = 1.96\pm 0.24$. All the measured quantities are in agreement with our QCD based Monte Carlo which uses the Lund model for hadronization. Finally, the ratio of $\bar{D}/D = 1.075\pm 0.021$ for $x_F > 0$, indicating that associated production is small at these energies, in contrast to the up to 70% effect seen at lower energies.^{11,12} Our results can be interpreted in the PGF model. We report on those investigations and on the studies of events with 2 reconstructed charm particles in a forthcoming paper.

We gratefully acknowledge the assistance of the staff of Fermilab and of all the participating institutions. This research was supported by the U. S. Department of Energy, by the Natural Science and Engineering Research Council of Canada through the Institute of Particle Physics, by the National Research Council of Canada and by the Brazilian Conselho Nacional de Desenvolvimento Científico e Tecnológico.

^aNow at Electro Magnetic Applications, Inc., Denver, CO, USA.

^bNow at Princeton University, Princeton, NJ, USA.

^cNow at CERN, Geneva, Switzerland.

^dDeceased.

^eNow at the University of Cincinnati, Cincinnati, OH, USA.

*Operated by the Universities Research Association, Inc. under contract with the United States Department of Energy.

¹ L. M. Jones, and H. W. Wyld, Phys. Rev. **D17**, 759 (1978).

M. A. Shifman, A. I. Vainstein and V. I. Zakharov, Phys. Lett. **65B**, 255 (1976).

² J. R. Raab et al., Phys. Rev. **D37**, 2391 (1988) and additional references therein.

³ S. D. Holmes, W. Y. Lee and J. E. Wiss, Ann. Rev. Nucl. Part. Sci. **35**, 397 (1985).

⁴ T. Sjöstrand, LU TP 85-10, University of Lund, Sweden.

⁵ D. O. Caldwell et al., Phys. Rev. Lett. **40**, 1222 (1978)

⁶ D. O. Caldwell et al., Phys. Rev. Lett. **42**, 553 (1979).

Refs. 5 and 6 report the total hadronic cross-section on H, C, Cu and Pb. The reported errors on the energy dependence of the hydrogen cross-section are included in the error on the energy dependence of our charm cross-section.

⁷ M. D. Sokoloff et al., Phys. Rev. Lett., **57**, 3003 (1986).

⁸ J. J. Aubert et al., Nucl. Phys. **B213**, 31 (1983).

⁹ G. D. Gollin et al., Phys. Rev. **D24**, 559 (1981).

¹⁰ J. Adler et al., Phys. Rev. Lett., **60**, 89 (1988).

J. Adler et al., Phys. Lett., **208B**, 152 (1988).

¹¹ K. Abe et al., Phys. Rev. **D37**, 1 (1986).

¹² M. I. Adamovich et al., Phys. Lett. **187B**, 437 (1987).

Figure Captions

1. The p_T^2 dependence of the cross-section on Be for all D mesons. The inner error is statistical, the outer error also includes in quadrature all systematic errors except those which affect only the overall scale. The fitted curve is described in the text.
2. The x_F dependence of the cross-section on Be for all D mesons. The inner error is statistical, the outer error also includes in quadrature all systematic errors except those which affect only the overall scale. The fitted curve is described in the text.
3. The E_γ dependence of the cross-section on Be for production of charm events ($\sigma_{c\bar{c}}$). The inner error is statistical, the outer error also includes in quadrature all systematic errors except those which affect only the overall scale. Also shown is a simple linear fit to the data points.

Particle	Mode	Raw Signal	R	Branching Ratio used(%)	σ on Be ($x_F > 0.2$)
D^0	$K^- \pi^+$	4252 ± 92	1.08 ± 0.03	$4.2 \pm 0.4 \pm 0.4^{10}$	$2.42 \pm 0.05 \pm 0.39 \mu\text{b}$
D^{*+}	$D^0 \pi^+$ $D^0 \rightarrow K^- \pi^+$	988 ± 34	1.15 ± 0.07	55.5 ± 4.5^{10} $4.2 \pm 0.4 \pm 0.4^{10}$	$1.37 \pm 0.05 \pm 0.25 \mu\text{b}$
D^{*+}	$D^0 \pi^+$ $D^0 \rightarrow K^- \pi^+ \pi^+ \pi^-$	1267 ± 47	1.23 ± 0.07	55.5 ± 4.5^{10} $9.1 \pm 0.8 \pm 0.8^{10}$	$1.60 \pm 0.06 \pm 0.31 \mu\text{b}$
D^+	$K^- \pi^+ \pi^+$	4864 ± 109	1.04 ± 0.03	$9.1 \pm 1.3 \pm 0.4^{10}$	$1.34 \pm 0.03 \pm 0.23 \mu\text{b}$

Table 1a. Cross-sections and antiparticle/particle ratios (R) for the high statistics modes. The cross-sections are the sum of the particle and antiparticle cross-sections.

Particle	Mode	Raw Signal	R	$\sigma \cdot \text{BR}$ on Be ($x_F > 0.2$)
D_s^+	$\phi \pi^+ + \bar{K}^{*0} K^+$	203 ± 17	0.92 ± 0.14	$25.0 \pm 2.2 \pm 1.9 \text{ nb}$
Λ_c^+	$p K^- \pi^+$	101 ± 13	0.79 ± 0.17	$40.4 \pm 5.4 \pm 5.1 \text{ nb}$

Table 1b. Cross-section times branching ratios and antiparticle/particle ratios (R) for the D_s^+ and Λ_c^+ . The $\sigma \cdot \text{BR}$ are the sum of the particle and antiparticle $\sigma \cdot \text{BR}$'s.

Particle	Mode	$\langle p_T^2 \rangle$	α in eqn. 2	n in eqn. 2	$\frac{\sigma(200GeV)}{\sigma(100GeV)}$
D ⁰	K ⁻ π ⁺	1.13±0.07	27±2	3.35±0.11	2.04±0.40
D ^{*+}	D ⁰ π ⁺	1.27±0.13	33±40	3.34±0.39	1.45±0.39
	D ⁰ → K ⁻ π ⁺				
D ^{*+}	D ⁰ π ⁺	1.27±0.16	8±1	2.66±0.48	2.37±0.65
	D ⁰ → K ⁻ π ⁺ π ⁺ π ⁻				
D ⁺	K ⁻ π ⁺ π ⁺	1.21±0.06	9±7	2.63±0.35	1.89±0.39
D ⁰ , D ⁺ mesons		1.16±0.04	14±10	2.95±0.22	1.96±0.24

Table 2. Results of fits to the p_T^2 , x_F and energy dependence for various modes. The errors on the parameters in the last 3 columns include systematic errors.

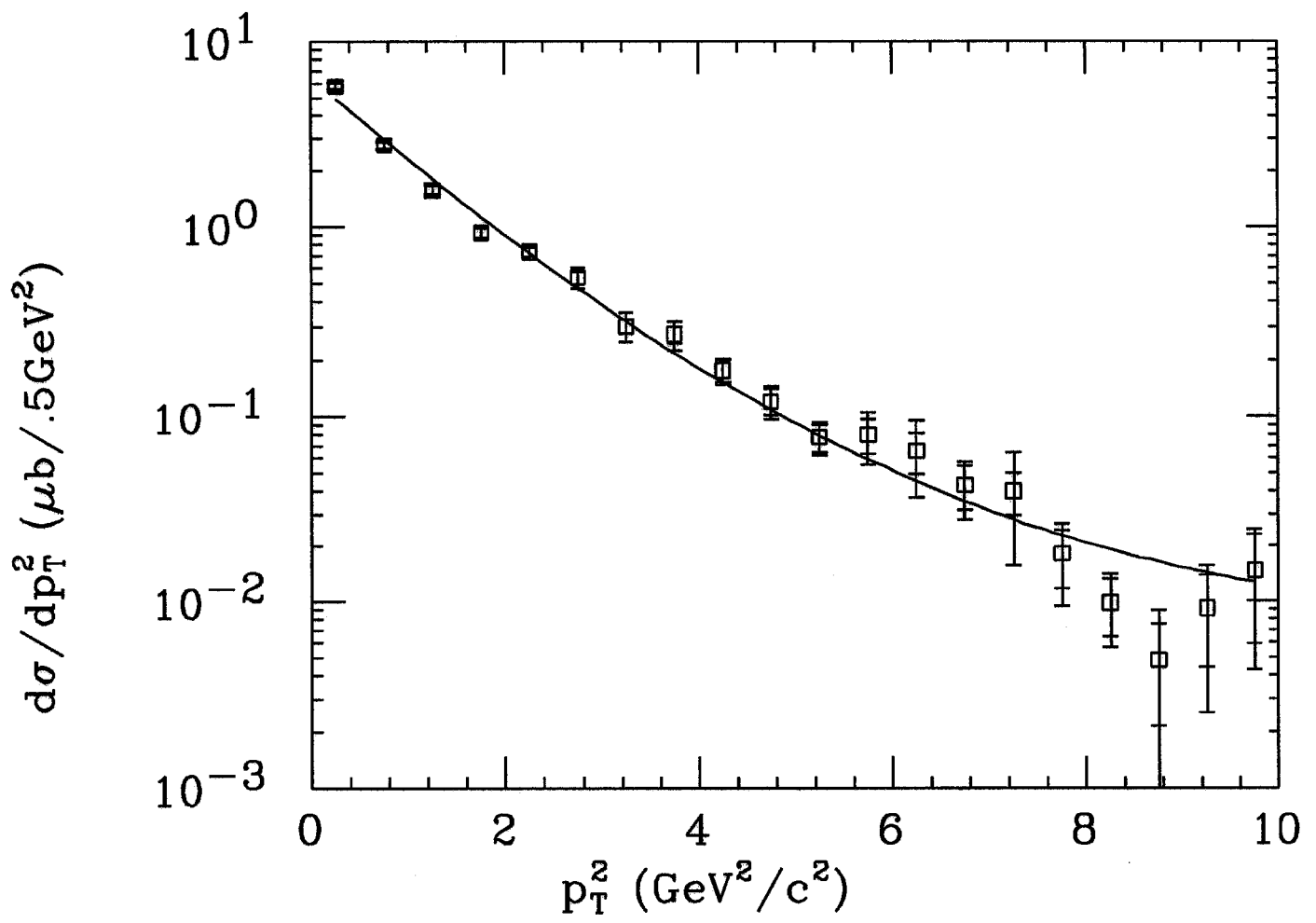


Figure 1.

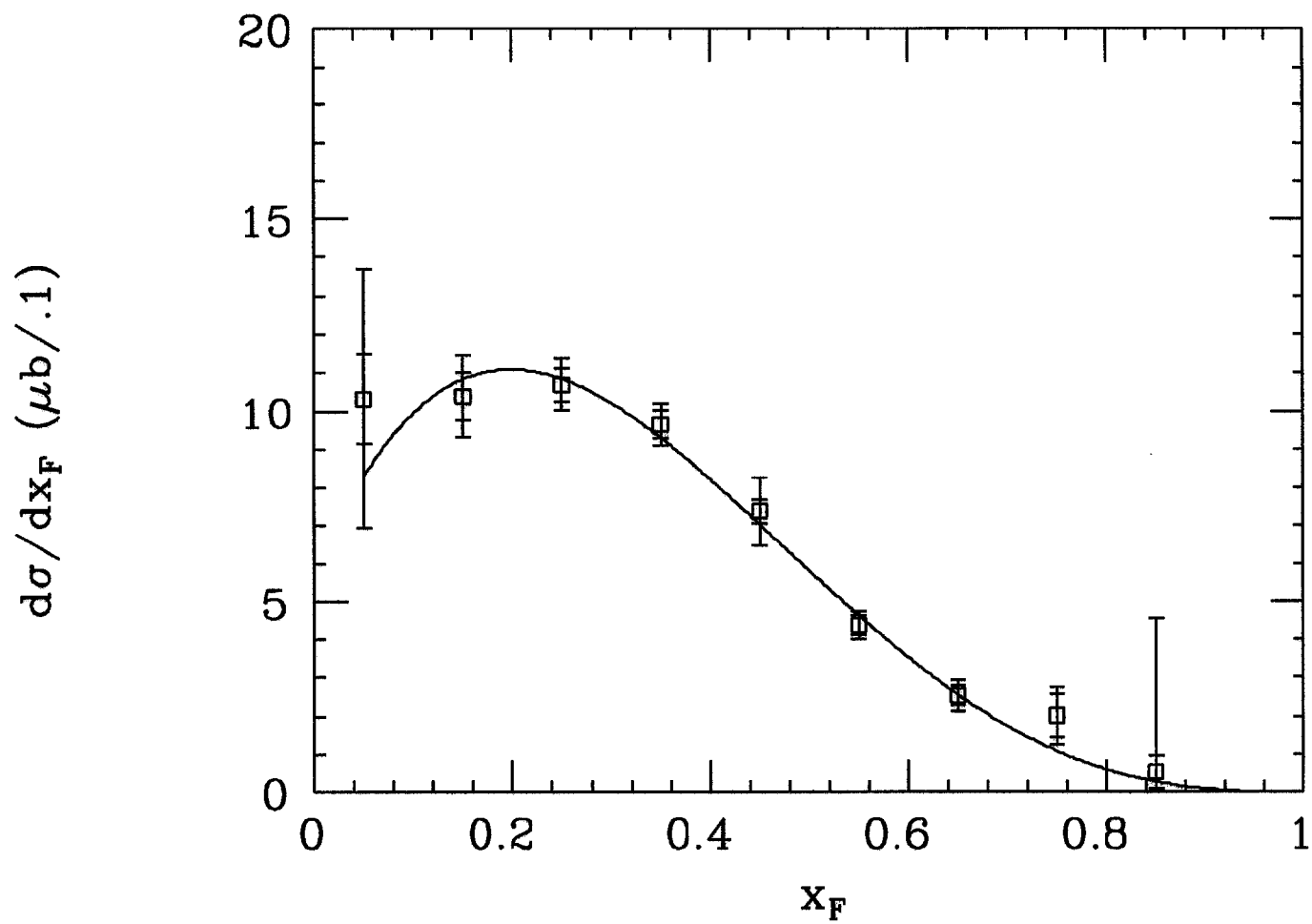


Figure 2.

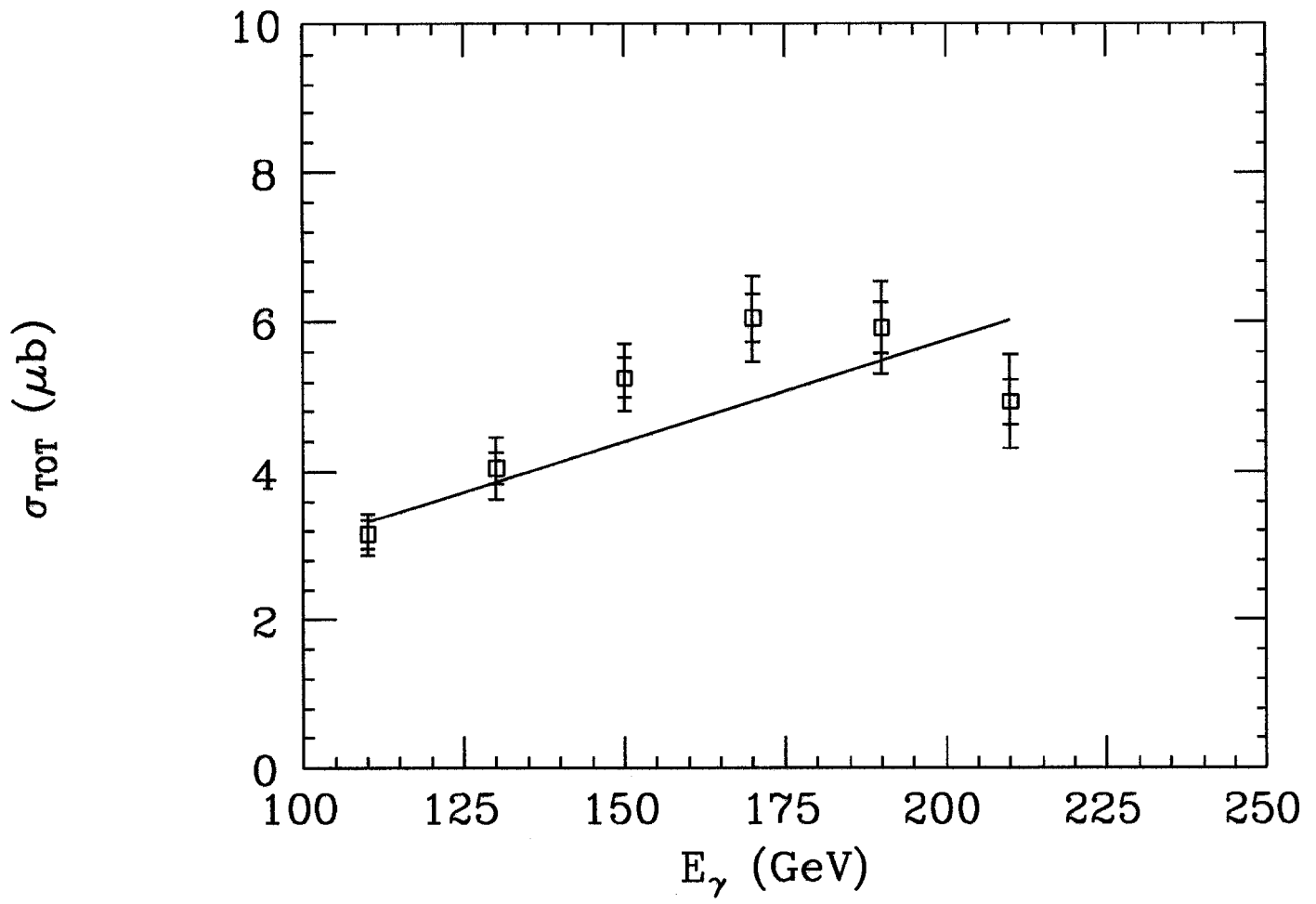


Figure 3.